DTP/00/109
hep-th/0012135

Looking for event horizons using UV/IR relations

James P. Gregory* **and Simon F. Ross†**

Centre for Particle Theory, Department of Mathematical Sciences
University of Durham, South Road, Durham DH1 3LE, U.K.

Abstract

A primary goal in holographic theories of gravity is to study the causal structure of spacetime from the field theory point of view. This is a particularly difficult problem when the spacetime has a non-trivial causal structure, such as a black hole. We attempt to study causality through the UV/IR relation between field theory and spacetime quantities, which encodes information about bulk position. We study the UV/IR relations for charged black hole spacetimes in the AdS/CFT correspondence. We find that the UV/IR relations have a number of interesting features, but find little information about the presence of a horizon in the bulk. The scale of Wilson loops is simply related to radial position, whether there is a horizon or not. For time-dependent probes, the part of the history near the horizon only effects the late-time behaviour of field theory observables. Static supergravity probes have a finite scale size related to radial position in generic black holes, but there is an interesting logarithmic divergence as the temperature approaches zero.

1 Introduction

Resolving the long-standing problems associated with black holes in quantum gravity seems to require a radical shift in our understanding of spacetime causal structure. Holographic theories of gravity, such as the AdS/CFT correspondence [1, 2, 3], seem to offer such a change in viewpoint. The true, fundamental causal structure of the theory is the fixed background causal structure in a d-dimensional field theory. The dynamical spacetime description is supposed to emerge from this underlying field theory in some approximation. Since spacetime has more dimensions than the space the field theory lives in, the encoding of information about the dynamical spacetime should be quite subtle. Understanding how the spacetime, especially its causal structure, are encoded in the field theory is one of the main open questions about these models. The aim of this paper is to see to what extent non-trivial causal structures, such as a black hole horizon, effect the values of simple gauge theory observables. We

*J.P.Gregory@durham.ac.uk
†S.F.Ross@durham.ac.uk

find that the causal structure near an event horizon does not appear in an obvious way in these observables.

In the AdS/CFT correspondence, the introduction of a source probe in the bulk will be reflected in a change in one-point functions in the field theory [4, 5, 6] (higher-point functions are also needed to resolve some probes; see e.g. [7, 8]). The holographic nature of the correspondence is reflected in a UV/IR relation between the radial position of the probe and the characteristic scale of the one-point function in the field theory [9, 10]. In the AdS_5/CFT_4 case, this can be expressed as a distance/distance relationship

$$\delta x_{\|} = \frac{\sqrt{g_{YM}^2 N}}{U} \tag{1}$$

(i.e., a source at radius U in AdS_5 corresponds to perturbing the field theory in a region of size $\delta x_{\|}$) [10]. Here, U is the radial coordinate in a Poincaré coordinate system, such that $U \to \infty$ at the boundary of AdS. Hence (1) relates large distances in spacetime (the IR) to short distances in the field theory (the UV).

In pure AdS_5, this relationship follows from the isometry $x^i \to \lambda x^i, U \to \lambda^{-1} U$ in the bulk. The UV/IR relationship has also been studied for more general metrics with Poincaré invariance in the directions parallel to the boundary. It is used to relate non-trivial solutions of this form to renormalization group flows in the dual field theory (a huge industry now; early works are [11, 12, 13, 14]). However, the class of spacetimes for which the description of bulk position in field theory terms is understood is still very limited. One of the goals of our paper is to attempt to extend the understanding of this relation for the simplest examples of spacetimes with a non-trivial causal structure.

In the relation (1), $U \to 0$ is mapped to diverging scale size in the field theory. From the spacetime point of view, $U = 0$ in Poincaré coordinates is an event horizon, and one can think of the divergence in the scale size as reflecting the one-way nature of the horizon: particles at the event horizon cannot move to larger U, and an infinite scale excitation can't return to smaller scale. As we will review in section 2, at least in pure AdS, the relation (1) provides a connection between spacetime and field theory causality throughout spacetime [15].

We would like to know if this connection between the UV/IR relation and causality can be generalised. A simple question to ask is whether the horizon of a black hole is also associated with an infinite scale size in the CFT. We will consider a variety of probes of black hole spacetimes, and find that the characteristic scale in the field theory description of time-independent probes is typically finite, even when they are very close to the horizon. Considering time-dependent probes is more complicated, but we argue that the scale size diverges at late times, although the leading behaviour is not directly related to the black hole structure.

The example that we study is a charged black hole in AdS. Considering charged black holes allows us to have a large separation between the horizon size and the thermal scale. In an uncharged black hole, the standard relation (1), and some probe calculations, would assign a scale size which is of the order of the thermal scale when a probe is at the black hole horizon. We would like to investigate if this connection

between the horizon and the thermal scale persists when there are other scales in the problem, or if we can see some sign of a divergent scale associated with the horizon. The presence of charge allows us to see which boundary scales are related to the thermal fluctuations in the gauge theory and which depend on the scale set by the black hole horizon.

The black holes we study are the toroidal "Reissner-Nordström AdS" black holes. In the case of AdS_5, these black holes can be obtained from the near horizon limit of spinning D3 branes [16]. Therefore the associated dual field theory is the world-volume theory on these branes. In [16, 17], the thermodynamic properties of charged Reissner-Nordström AdS_{n+1} black holes was investigated. They considered both spherical black holes, with the boundary $\mathbf{R} \times S^{n-1}$, and toroidal black holes, where the asymptotic boundary is $\mathbf{R}^n$. From the point of view of thermodynamics, the spherical black holes are more interesting, but to analyse UV/IR relations, we will focus on the simpler case of toroidal black holes. These can be obtained as the infinite volume limit of the spherical black holes. The metric for these black holes is

$$ds^2 = -V(U)dt^2 + \frac{dU^2}{V(U)} + \frac{U^2}{R^2}\sum_{i=1}^{n-1} dx_i^2, \tag{2}$$

where

$$V(U) = \frac{U^2}{R^2} - \frac{m}{U^{n-2}} + \frac{q^2}{U^{2n-4}}. \tag{3}$$

We work in units where $l_s = 1$, so $R = (g_{YM}^2 N)^{1/4}$. The horizon radius, U_T, is given by $V(U_T) = 0$, and the temperature T is related to the period β in Euclidean time by

$$\beta = \frac{1}{T} = \frac{4\pi}{V'(U_T)} = \frac{4\pi R^2 {U_T}^{2n-3}}{n{U_T}^{2n-2} - (n-2)q^2R^2}. \tag{4}$$

The black hole will be extremal ($T = 0$, and the horizons coincide) at $U_T = U_e$, where ${U_e}^{2n-2} = (n-2)R^2q^2/n$. It was shown in [16] that these black holes are thermodynamically stable (in both the canonical and the grand canonical ensembles) for arbitrary values of the mass and charge, so the black hole solutions carry information about the CFT in the corresponding ensemble. We will focus on the case of AdS_5, that is, $n = 4$.

It was further shown in [18] that the spherical black hole solutions in the $AdS_5 \times S^5$ context will not have superradiant modes, as the internal S^5 rotates at a speed less than the speed of light everywhere in the spacetime. It is easy to extend their argument to the toroidal black holes. The charged black hole (2) is derived from the reduction ansatz

$$ds^2 = g_{\mu\nu}dx^\mu dx^\nu + \sum_{i=1}^{3}\left[d{\mu_i}^2 + {\mu_i}^2\left(d\phi_i + A_\mu dx^\mu\right)^2\right] \tag{5}$$

where $g_{\mu\nu}$ is the five-dimensional metric, μ_i are the direction cosines and ϕ_i are the rotation angles on the S_5. Non-zero A_t gives the electric potential

$$A = (\Phi(U_T) - \Phi(U))dt, \text{ where } \Phi(U) = \frac{q}{U^2} \tag{6}$$

The norm of the Killing vector field $k = \partial/\partial t$ with respect to our ten dimensional metric is

$$k^2 = -\left(1 - \frac{{U_T}^2}{U^2}\right)\left[U^2\left(1 - \frac{{U_-}^2}{U^2}\right) + \left(1 - \frac{{U_-}^2}{{U_T}^2}\right)({U_T}^2 + {U_-}^2)\right], \tag{7}$$

where U_- is the inner horizon. We see that k^2 is always negative outside the black hole horizon, and thus superradiance cannot occur for the toroidal black hole.

A useful rewriting of the metric (2) is

$$ds^2 = \frac{R^2}{U^2}\frac{dU^2}{f(U)} + \frac{U^2}{R^2}\left[-f(U)dt^2 + \sum_{i=1}^{3} {dx_i}^2\right], \tag{8}$$

$$f(U) = 1 - (1+\theta)\frac{{U_T}^4}{U^4} + \theta\frac{{U_T}^6}{U^6}, \tag{9}$$

where we have defined a dimensionless parameter $\theta = q^2R^2/{U_T}^6$; for the uncharged black hole $\theta = 0$, while the extremal black hole has $\theta = 2$. The case $\theta = U_T = 0$ is pure AdS_5 in Poincaré coordinates, where (1) is valid.

After reviewing the connection between (1) and causality in section 2, we move on to consider specific probes in this black hole background. We begin with a discussion of Wilson loops in section 3. We find that the qualitative behaviour of the loop expectation values is independent of the charge, and the non-trivial physics associated with the presence of a black hole appears at a scale given by (1). That is, the characteristic scale for these observables is the inverse horizon size, and is not in general related to the temperature. We then go on to discuss supergravity probes in section 4. We find that the scale of the expectation value for time-dependent probes diverges at late times, but the expectation value is primarily determined by the asymptotic metric. We study the small contribution from the near-horizon region in the BTZ metric, and argue that it is spatially constant. For static supergravity probes, there is a finite scale size associated with the horizon in general. The scale size associated with the static propagator diverges like $\ln(T)$ in the extremal limit $T \to 0$. This behaviour provides the main element of surprise in the paper, and it would be very interesting to gain a better understanding of this logarithmic dependence from the field theory point of view.

In addition to addressing the implications for our understanding of bulk causality, we will briefly comment on the physical significance of these UV/IR relations from the field theory point of view, and remark on the relation to previous work [19, 20] which studied the Euclidean rotating brane solutions as models for pure gauge theories.

We conclude in section 5 with a discussion of the difficulties in identifying the origins of spacetime causal structure in the gauge theory, and some speculations for future directions.

2 UV/IR relations in black hole spacetimes

To begin our investigation of the UV/IR relation in spacetimes with horizons, we review the connection between the UV/IR relation and causality in pure AdS proposed

in [15]. In pure AdS, the condition for a bulk probe to move inside the light cone in the radial direction is

$$-\frac{U^2}{R^2}dt^2+\frac{R^2}{U^2}dU^2\leq 0. \tag{10}$$

For a supergravity probe, the UV/IR relation (1) implies that (10) is equivalent to

$$\left|\frac{d\delta x_\parallel}{dt}\right|\leq 1, \tag{11}$$

which is just the statement that the field theory excitation's size cannot change faster than the speed of light in the field theory. This thus connects the causality of AdS to the causality of the space the field theory lives in.

It would be interesting to see if a similar relation could exist for black hole spacetimes, through a suitable modification of the UV/IR relation (1). In a black hole spacetime, the condition (10) is modified to

$$-\frac{U^2}{R^2}f(U)dt^2+\frac{R^2}{U^2f(U)}dU^2\leq 0. \tag{12}$$

We could derive a candidate UV/IR relation on the black hole spacetime by assuming that this spacetime condition is still equivalent to the kinematical condition (11). If we assume a UV/IR relationship of the form $\delta x_\parallel = g(U)$, then (11) would imply

$$\left|\frac{dU}{dt}\right|\leq\left|\frac{dU}{dg(U)}\right|. \tag{13}$$

Requiring that this condition is equivalent to (12) gives

$$\left|\frac{dg(U)}{dU}\right|=\frac{R^2}{U^2f(U)}. \tag{14}$$

This can be solved exactly for the black hole spacetimes we are considering, but the important feature is how the boundary scale size behaves for a probe near the black hole horizon. The behaviour differs according to whether or not the black hole is extremal, but in both cases the scale size becomes infinite as the black hole horizon is approached.

$$\theta\neq 2 \;\;\Rightarrow\;\; \delta x_\parallel\sim\frac{R^2}{2(2-\theta)}\ln(U-U_T), \tag{15}$$

$$\theta=2 \;\;\Rightarrow\;\; \delta x_\parallel\sim\frac{R^2}{12}\frac{1}{U-U_T}. \tag{16}$$

Thus, a diverging scale size for probes at finite radial position would be a signature of a horizon, under the assumption that bulk causality arises from a kinematical restriction in the field theory. This is the main prediction we will investigate in our discussion of the probes.

In studies of the uncharged black holes, it was found that sources near the black hole horizon produced expectation values with a scale $\delta x_\parallel\sim 1/T$, where T is the

temperature [4, 21, 22]. It was proposed that the physical interpretation of this is that probes which fall into the horizon become entangled with the thermal bath in the gauge theory. This suggests that the presence of finite-temperature Hawking radiation acts as a barrier to our ability to probe the non-trivial classical causal structure in the region near the horizon. One reason for our extension to the charged black holes is that it enables us to consider black holes of arbitrarily low temperature, and separate the thermal scale from the horizon radius, allowing us to study this issue further.

3 Wilson loop calculations

The expectation value of a Wilson loop operator in the field theory is related by the AdS/CFT correspondence to the action for a string worldsheet in the bulk which terminates on the path of the Wilson loop on the boundary [23, 24]. This makes this a very convenient observable to consider, as we can investigate its leading-order behaviour by finding the minimal-area surface for the string worldsheet. The symmetries of the metric (8) lead us to consider rectangular Wilson loops with two long sides, and a separation L between them. The long sides lie either along the t direction (timelike Wilson loops) or along one of the x^i directions (spacelike Wilson loops).

3.1 Timelike Wilson Loops

We wish to consider Wilson loop operators in the boundary theory, where the loop $\mathcal{C}$ forms a rectangle with two long sides extended along the t direction, of length t_0, and two sides of length L along one of the x^i directions. From the field theory point of view, the value of this operator determines the potential of an external quark-antiquark pair. This potential was obtained in [23, 24] for the vacuum (pure AdS). The expectation value of the Wilson loop behaves like $\langle W(\mathcal{C})\rangle \sim \exp(-t_0 E)$ in the limit $t_0 \to \infty$, where $E = V(L)$ is the lowest possible energy of the quark-antiquark configuration. For large N and large $g^2_{YM}N$, this expectation value is given by $\langle W(\mathcal{C})\rangle \sim \exp(-S)$, where S is the Nambu-Goto action for a fundamental string worldsheet which joins the boundary at the loop $\mathcal{C}$ (we must also subtract the infinite mass of the W-boson to regularize this supergravity calculation). This calculation was extended to the field theory at finite temperature by considering a string worldsheet in a Schwarzschild-AdS background in [22, 21][1]. In pure AdS, the quark-antiquark potential is $V \propto -(g^2_{YM}N)^{1/2}/L$, as expected by conformal invariance. At finite temperature, the small-L behaviour is similar, but screening sets in and $V = 0$ at $L \sim 1/T$, where T is the temperature.

Our objective is to investigate the quark-antiquark potential obtained from the string worldsheet in the charged AdS black hole background. We begin with the metric (8), and calculate the string worldsheet area from the Nambu-Goto action

$$S = \frac{t_0}{2\pi}\int dx \sqrt{(\partial_x U)^2 + \frac{U^4}{R^4} f(U)}. \tag{17}$$

[1] A review of Wilson loops from the string/gauge correspondence can be found in [25] which includes extensive references.

We are working in the static gauge $\tau = t$, $\sigma = x$ for the string worldsheet coordinates, where x is the position in the boundary direction along which the quarks are separated. This action is independent of x, so we can calculate x from the Euler-Lagrange equations to find

$$x = \frac{R^2}{U_T}\alpha\sqrt{1-(1+\theta)\alpha^4+\theta\alpha^6}\int_1^{\frac{U_\alpha}{U_T}} \frac{y^2 dy}{\sqrt{(y^2-1)(y^2-\alpha^2)(y^4+\alpha^2y^2-\theta\alpha^4)(y^4+y^2-\theta\alpha^6)}}. \tag{18}$$

We have introduced a dimensionless parameter $\alpha = U_T/U_0$, where U_0 is the minimum value of the radial coordinate along the string worldsheet in AdS. We see that $x = 0$ at $U = U_0$, so the string profile is symmetric about $x = 0$. Furthermore, the separation of the quarks is given by $L = 2x(U = \infty)$. We wish to calculate the energy, which is naïvely given by S/t_0, where S is the action (17) integrated over the range $-L/2 \leq x \leq L/2$. However, as was pointed out in [23, 24] and subsequent works, this would give an infinite result due to the contribution from the mass of the W-boson. We must therefore regularize the expression by only integrating up to $U = U_{max}$, and subtracting the regularized mass of the W-boson, $U_{max}/(2\pi)$. Taking our cutoff to infinity, we then find the solution for the energy

$$E = \frac{U_T}{\pi\alpha}\left[\int_1^\infty \left(\frac{\sqrt{(y^2-\alpha^2)(y^4+\alpha^2y^2-\theta\alpha^4)}}{\sqrt{(y^2-1)(y^4+y^2-\theta\alpha^6)}} - 1\right)dy - 1 + \alpha\right]. \tag{19}$$

We can only evaluate this integral by numerical methods. If we plot E/U_T against LU_T/R^2, the only free variable is θ, which specifies the charge on the black hole. We can study the effect of the charge by varying θ. The results obtained in the uncharged case have been reproduced here for comparative purposes in figure 1. The typical behaviour of E vs. L for a charged black hole (plotted here is the case $\theta = 1$) is given in figure 2, and the behaviour for the extremal black hole is given in figure 3. It should be noted that in these plots the parameter α is not plotted over the complete range, as numerical methods to solve the integral break down when α is close to 0 or 1. However, the behaviour of the E vs. L plot in the unplotted regions can be observed from studying L and E separately as functions of α. As $\alpha \to 0$, $L \to 0$ and $E \to -\infty$. With α increasing from 0, the E vs. L plot rises smoothly to the cusp with increasing L and increasing E, at which point both L and E begin to decrease along the upper branch. This monotonic decreasing behaviour in L and E continues until $\alpha = 1$ where both L and E are zero.

In the uncharged case, it was remarked that the upper branch (with $E \geq 0$) is unphysical. The potential energy shown in the graph is the energy of a U-shaped string configuration hanging into the bulk. There is an alternative configuration, a pair of strings hanging straight down to the horizon. This second configuration has zero energy (after we subtract the W-boson mass contribution), so when the energy of the U-shaped configuration is greater than zero, this configuration is no longer energetically favourable and we pass over to the other. We should therefore only consider the section of the E vs. L curves with negative energy. Where the curve crosses the axis, the potential becomes constant. From the point of view of gauge

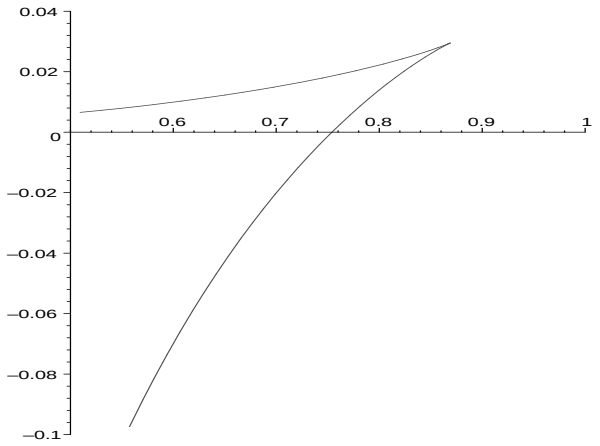

Figure 1: E vs. L plot for uncharged black hole ($\theta = 0$)

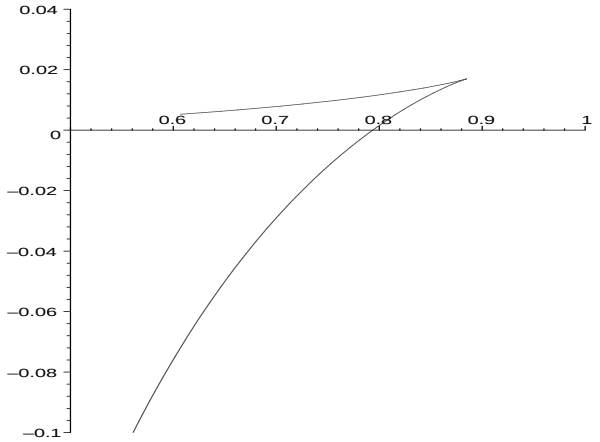

Figure 2: E vs. L plot for charged black hole ($\theta = 1$)

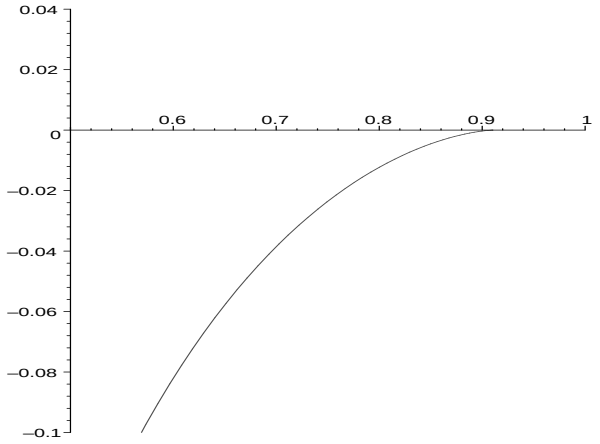

Figure 3: E vs. L plot for extremal black hole ($\theta = 2$)

theory, this corresponds to the screening of the quark charge by the plasma in the field theory which carries the energy of the thermal state.

We see that the qualitative behaviour of the potential remains the same as the charge of the black hole is increased. The separation at which screening sets in increases slightly, but the overall scale is still set by the horizon radius U_T. This is reasonable from the point of view of the field theory, since we interpret this screening as due to polarization in the plasma in the field theory which carries the energy density in this state (which corresponds to the black hole mass from the spacetime point of view). In the charged black hole case, this energy density goes like U_T, and not like the temperature. Even in the extremal, $T \to 0$ limit, there is still a finite energy density, which is responsible for the screening behaviour in figure 3.

It is interesting to observe that the maximum value of the parameter α for which E is negative increases from ~ 0.66 in the uncharged case to 1 in the extremal charged case. That is, as we increase the charge, the string worldsheet probes deeper into the interesting region near the horizon before the cross-over to the disconnected solution. Despite this behaviour, these loops are not a good probe of the bulk causality. In particular, there is no sign of any special behaviour as $T \to 0$. From the field theory point of view, the qualitative screening behaviour is associated with the background energy density, and one seems to find qualitatively similar behaviour independent of the details of the energy distribution. It is also possible to construct examples which display the same screening behaviour without a black hole horizon, for example by considering states on the Coulomb branch of the field theory [26, 27, 8]. Thus, while the value of the screening length is dictated by the horizon radius U_T, this probe is insensitive to the horizon as a horizon.

3.2 Spacelike Wilson Loops

We can use similar techniques to study spacelike Wilson loops. Spacelike Wilson loops for the finite temperature field theory were considered in [28, 29]. In the uncharged case, one could consider the Euclidean AdS Schwarzschild black hole, and analytically continue one of the spatial x^i directions instead of the time t. Because of the thermal boundary conditions, the t direction is compactified on a circle of period $\beta = 1/T$ in the Euclidean solution. At energies smaller than the compactification scale, we should obtain a pure gauge theory living in the $2+1$ uncompactified directions, as all the other modes of the original theory get a mass proportional to the temperature. The spacelike Wilson loop with the long side along the analytically continued direction is interpreted as giving the quark-antiquark potential in this gauge theory. The supergravity calculation indicated that it would display an area-law behaviour for $L \gg \beta$, in agreement with the expectation that this pure Yang-Mills theory is confining. Unlike the timelike loops, the string worldsheet always approaches arbitrarily close to the horizon as we increase the separation in the boundary.

In the charged case, the spacelike Wilson loop determined by string worldsheets in the metric (8) does not have the same interpretation. To get a real Euclidean solution from (8), we need to analytically continue both $t \to i\tau$ and $q \to iq'$. (This is easy to see if we remember that this charge comes from rotation in the higher-

dimensional solution; that is, it is an angular momentum parameter.) This analytic continuation drastically changes the physics–for example, the analytically continued metric no longer has an extremal limit–and calculations of the spacelike Wilson loops in the Lorentzian metric (8) are therefore not simply related to the properties of a $2+1$ pure gauge theory. Our motivation for studying the spacelike Wilson loops is thus simply that they are an interesting probe of the state in the 3+1 supersymmetric field theory corresponding to our charged black holes.

The action for the string worldsheet spanning a loop along two spatial dimensions is

$$S = \frac{Y}{2\pi}\int dx\sqrt{\frac{(\partial_x U)^2}{f(U)}+\frac{U^4}{R^4}}, \tag{20}$$

where Y is the length of the long side of the loop. Repeating the method of calculation of L and E used above, we find

$$L = \frac{2R^2\alpha}{U_T}\int_1^\infty \frac{ydy}{\sqrt{(y^4-1)(y^2-\alpha^2)(y^4+\alpha^2y^2-\alpha^4\theta)}}, \tag{21}$$

$$E = \frac{U_T}{\pi\alpha}\left[\int_1^\infty\left(\frac{y^5}{\sqrt{(y^4-1)(y^2-\alpha^2)(y^4+\alpha^2y^2-\alpha^4\theta)}}-1\right)dy-1+\alpha\right]. \tag{22}$$

We would like to find the behaviour of the theory at large L. L is increasing as a function of α, so this requires us to consider the behaviour for $\alpha\to 1$ (i.e., we consider strings which hang close to the horizon). For any value of the parameter θ, both of the integrals are then dominated by the region $y=1$. So for $\alpha\to 1$, the integrals in L and E become the same and we uncover the same area law as in the uncharged case:

$$E = \mathcal{T}L, \tag{23}$$

where the tension $\mathcal{T}=\frac{U_T^2}{2\pi R^2}$. The E vs. L plot for the extremal black hole is given in figure (4), to illustrate the similarity with the uncharged case. The scale at which the linear behaviour sets in is once again determined primarily by the horizon radius U_T; the effect of θ is just some multiplicative factor of order unity.

These probes see the horizon basically as a boundary, providing a lower bound on $g_{x^ix^i}$, and hence enforcing an area law behaviour at large distances. Since they don't probe the g_{tt} part of the metric, it is not suprising that they're not good probes of the causal structure, or particularly sensitive to the temperature.

4 Supergravity probes

We now consider the supergravity propagators on the charged black hole background. These can be used to calculate the dual expectation value for sources coupled to the supergravity fields near the horizon. One might hope that these supergravity sources will better probe the causal structure, as unlike the string worldsheets considered above, these sources can have compact support in the radial direction. However, the

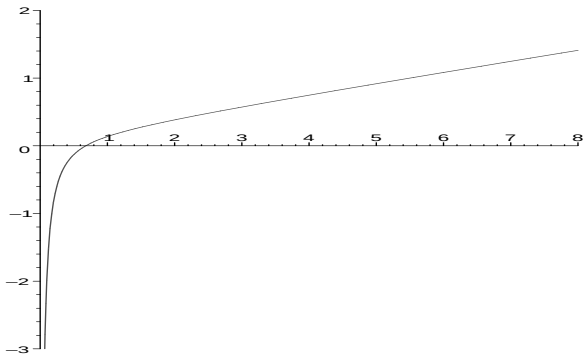

Figure 4: Spacelike Wilson loop - E vs. L plot for extremal black hole. As before, we plot E/U_T against LU_T/R^2.

fact that the one-point functions are determined by the asymptotic fields will still complicate the story.

4.1 Retarded propagator

We consider first the retarded propagator, defined as the solution to the wave equation

$$\partial_\mu(\sqrt{-g}g^{\mu\nu}\partial_\nu G(x,x')) = \delta(x-x') \tag{24}$$

subject to the boundary condition $G(x,x') = 0$ for $t < t'$. Here, x' is the position of the source, and x is the position where the measurement is made. It is natural to assume that sources in the bulk will follow geodesics, and in the charged black hole spacetimes, this implies that they will fall into the black hole. To study the effects of such source probes, we must calculate boundary expectation values using the retarded propagator; to learn about the causal structure, we must respect it. Unfortunately, explicit calculations are extremely difficult, except in 2+1 dimensions, where the black hole is locally AdS. We will remark on the qualitative features of geodesic probes, assuming the solution has similar properties to the solution in pure AdS.

The retarded propagator in pure AdS was previously investigated in [30], where an explicit solution was constructed. In AdS_{2n+1}, the retarded propagator is non-zero only in the part of the forward light cone that can be reached by a causal geodesic. In AdS_{2n}, it is non-zero only on the forward light cone. In either case, the retarded propagator from a point in the bulk to a point on the boundary is non-zero only where the forward light cone of the point in the bulk intersects the boundary.

The expectation values dual to probes following geodesics in pure AdS were constructed in [30]. There is an isometry which maps any geodesic in pure AdS to any other, which acts on the boundary as a conformal transformation. This can be used to obtain the expectation value dual to a boosted probe. These geodesics start from large radius in the Poincaré coordinates and fall towards the horizon. As the boost is increased, the initial position is moved to larger radius, bringing the probe closer to the boundary. It was found that as the boost is increased, the expectation value

became concentrated in a 'bubble' around the light-cone of the point where the source makes its closest approach to the boundary (see [30] for details). An exact metric describing a lightlike particle falling from a point on the boundary of AdS was found in [31]. In that case, the dual expectation value was a delta-function along the light cone of the point on the boundary that the particle fell from, in agreement with the general arguments for test particles. Thus, the expectation value spreads to infinite scale size as the particle falls towards the horizon. (Note that for a time-dependent probe, we have to wait for an infinitely long time to see this infinite scale size, which makes this a little inconvenient as a probe of causality.)

Thus, most of the expectation value is along the light cone of the initial point when the source starts near the boundary. By causality, only the part of the source trajectory near the boundary can be contributing to this part of the expectation value; the region where the expectation value is large is outside of the light cone of all but the initial part of the probe's trajectory. Thus, in pure AdS, the expectation value lies mostly in an expanding bubble around the initial point, and is determined by the part of the source trajectory at large radial distances.

This has several lessons for the black hole spacetimes. In black hole spacetimes, the metric at large distances is approximately AdS, so we would expect propagation in this region to be well-approximated by the propagation in pure AdS. Thus, for a source starting at large radial distance in the black hole geometry, the expectation value will have a contribution which produces a delta-function along the light cone. This part will spread out to infinite scale size along the light cone, just as it did in AdS. In an uncharged black hole background, there are thermal fluctuations around this average value, so it was argued in [4] that in practice, we will see the the bubble expand until it reaches the thermal scale, where it becomes confused with the thermal fluctuations. In the charged black hole, we can suppress these thermal fluctuations, so we should be able to see the bubble expanding to larger and larger scales, just as in pure AdS.

Although it is tempting to see this as a sign that the horizon is associated with infinite scale size, we should note that this expansion of the bubble is not connected with the horizon in the interior; it is determined by the behaviour of the probe far from the horizon. To see the effects of the non-trivial causal structure, we should consider the contribution to the expectation value from the region near the horizon. Because of the non-trivial causal structure, there can be a contribution from the region near the horizon only at very late times. Furthermore, the discussion in pure AdS suggests this contribution will be very small.

If we consider the BTZ black hole in AdS_3, we can study the propagator from the near-horizon region, since the spacetime is locally pure AdS. The metric is [32]

$$ds^2 = -\frac{(r^2 - r_+^2)}{\ell^2} dt^2 + \frac{\ell^2 dr^2}{(r^2 - r_+^2)} + r^2 d\phi^2, \tag{25}$$

where ℓ (the analogue of R in our higher-dimensional discussion) is the cosmological length scale. If ϕ ranges over all values, this is a peculiar coordinate system for AdS_3. If ϕ is periodically identified with period 2π, this is a black hole with a horizon at

$r = r_+$. A lightlike geodesic starting at the boundary point $t = 0, \phi = 0$ is described by

$$\phi = 0, r = r_+ \coth \frac{t r_+}{\ell^2}. \tag{26}$$

The propagator from a point on this trajectory to the boundary at $r = \infty$ will be non-zero only at the intersection of the light-cone of the point with the boundary (since the space is locally AdS, we can use the propagator obtained in [30]). For a point at $r = r_+(1+\epsilon)$, the light cone meets the boundary at

$$t \approx \frac{\ell^2}{r_+} \ln \left(\frac{2\cosh(r_+\phi/\ell)}{\epsilon} \right). \tag{27}$$

As expected, t here goes to infinity as the source approaches the horizon. More importantly, the point contributes at later times as we increase ϕ. We consider the contribution to the expectation value at some fixed late time from the source worldline near the horizon. If we take the source sufficiently close to the horizon, we need only consider the contribution from the source at $\phi = 0$, and not that of the images under the identification at $\phi = \pm 2\pi n$. That is, we can disregard the compactification of ϕ for this calculation.

The expectation value for a geodesic source in these coordinates with $\phi \in (-\infty, \infty)$ is [30]

$$\langle \mathcal{O} \rangle = \frac{(a r_+)^\Delta}{(a^2 + (1+a^2)\sinh^2[r_+(t+\phi)/2])^{\Delta/2} (a^2 + (1+a^2)\sinh^2[r_+(t-\phi)/2])^{\Delta/2}} \tag{28}$$

for an operator of conformal dimension Δ, where a is the boost parameter (the source is lightlike for $a \to 0$). This expectation value is approximately independent of ϕ for $\phi \in (-\pi, \pi)$ at large t. Thus, the contribution to the expectation value from the region near the black hole horizon is ϕ-independent, which is as close as we can come to infinite scale in the present context of a compact spatial direction on the boundary. We reiterate that this is just the contribution from the region near the horizon; the main contribution to the expectation value is at $t = \pm\phi$ as discussed in [7], and comes from the part of the worldline near the boundary.

4.2 Static propagator

We will next turn to static sources. The advantage of considering static sources is that since the source is always near the horizon, the expectation value will be affected by the near-horizon structure. However, the static propagator is independent of g_{tt}, so this is not guaranteed to produce a result which reflects the causal structure near the black hole, and in fact the answer we obtain does not have a straightforward relation to statements about the causality. However, it does appear to encode information about the near-horizon region in a non-trivial way.

The calculation of the appropriate propagator in the uncharged black hole background was discussed in [30]. The static propagator for a massless scalar field is

defined as a solution to the equation

$$\partial_i \left(\sqrt{g} g^{ij} \partial_j G(x, x') \right) = \sqrt{g_{tt}} \delta(x - x'). \tag{29}$$

Here x' is the position of the source, while x is the point at which the field is measured. We take the metric (8) and rescale the coordinates by $U \to U_T u$, $t \to t R^2/U_T$ and $x \to x R^2/U_T$. The equation for the static propagator is then

$$\begin{aligned} \left(u^7 - (1+\theta)u^3 + \theta u \right) \partial_u^2 \tilde{G} + \left(5u^6 - (1+\theta)u^2 - \theta \right) \partial_u \tilde{G} - u^3 k^2 \tilde{G} \\ = \frac{\sqrt{u^6 - (1+\theta)u^2 + \theta}}{R^7} \delta(u - u'). \end{aligned} \tag{30}$$

Here we have Fourier transformed the propagator equation with respect to x_i, so

$$\tilde{G}(u, u', k_i) = \int d^3k e^{i\vec{k}\cdot\vec{x}} G(u, u', x_i). \tag{31}$$

For $u < u'$ and $u > u'$ the Green's function is given by the solutions of the homogeneous equation

$$\left(u^7 - (1+\theta)u^3 + \theta u \right) y''(u) + \left(5u^6 - (1+\theta)u^2 - \theta \right) y'(u) - u^3 k^2 y(u) = 0. \tag{32}$$

We must now consider the indicial equations which arise for solutions near the horizon $u = 1$ and the boundary $u = \infty$. For $u > u'$ this is $\sigma^2 + 4\sigma = 0$, and the presence of electric charge makes no difference to the boundary behaviour of the Green's function. In order for the solution to vanish at infinity, as required, we therefore have

$$\tilde{G}(u > u', k) = A y_1(u, k) \text{ where } y_1(u, k) \sim \frac{1}{u^4}, u \to \infty. \tag{33}$$

For the behaviour near $u = 1$, we have the indicial equation $(4 - 2\theta)(\sigma(\sigma - 1) + \sigma) = 0$. So long as $\theta \neq 2$ (i.e., for a nonextremal black hole) this is also the same as in the uncharged case, and regularity at the horizon requires

$$\tilde{G}(u < u', k) = B y_2(u, k) \text{ where } y_2(u, k) \sim 1, u \to 1. \tag{34}$$

We will return to the extremal case later in this section. The constants A and B are calculated by continuity in the Green's function at $u = u'$ and the correct discontinuity in its derivative, giving

$$A = \frac{y_2}{W(y_1, y_2)} \frac{1}{R^7 u' \sqrt{u'^6 - (1+\theta)u'^2 + \theta}}, B = \frac{y_1}{W(y_1, y_2)} \frac{1}{R^7 u' \sqrt{u'^6 - (1+\theta)u'^2 + \theta}}. \tag{35}$$

From (32) we see that the the Wronskian $W(y_1, y_2)$ is

$$W(y_1, y_2) = \frac{w(k)}{u^5 - (1+\theta)u + \frac{\theta}{u}}. \tag{36}$$

The value of the dilaton can then be computed as in [30]. The position-space propagator is written as the Fourier transform of this momentum-space propagator, and the integrals in this Fourier transform are expressed as a sum over the poles of $\tilde{G}(u, u', k_i)$. The boundary behaviour of the dilaton field is then found to be

$$\phi(U,x) \overset{U\to\infty}{\approx} \frac{{U_T}^4}{8\pi R^6 U^4} \sum_{n=1}^{\infty} \frac{e^{-m_n r}}{m_n r w'(m_n)} \int du' y_2(u', m_n) du'. \tag{37}$$

Here, m_n are the zeros of $w(k)$, which give poles in the propagator. These correspond to the special values of k for which we can construct solutions regular at both the horizon and infinity. $y_2(u', m_n)$ are the corresponding solutions of equation (32). Thus, the propagator has an exponential suppression for $r > 1/m_n$, and these poles hence provide a maximum length scale for the expectation value dual to sources anywhere in the bulk. We proceed to determine this maximum scale by finding the poles m_n.

In the case of the uncharged black hole, this problem of determining the zeros of the Wronskian physically corresponded to finding the glueball mass spectrum for the $2+1$ dimensional pure Yang-Mills theory, and was first described in [28], and both numerical methods and analytic approximations have since been used to calculate the spectrum [33, 34, 30]. As was emphasised in the discussion of spacelike Wilson loops, the Lorentzian metric (8) is not directly related to the $2+1$ field theory obtained from a Euclidean rotating brane metric. Thus, the zeros m_n found here will not be simply related to the glueball mass spectra obtained from studies of the rotating brane metrics in [19, 20].

We follow the approach of [34] in calculating m_n, as the change of coordinates employed there makes the interpretation in the extremal limit clear. Returning to equation (32), with the change of variables $x = u^2$ ($k = i\kappa$), we find

$$\partial_x \left[(x^3 - (1+\theta)x + \theta) \partial_x y \right] + \kappa^2 y = 0. \tag{38}$$

In order to use WKB methods on a second order linear differential equation, it is necessary to redefine the dependent variable so that it satisfies a differential equation with no first derivative term. The WKB analysis is greatly simplified with the change of variables $x = 1 + e^z$. Defining

$$\psi = \sqrt{\frac{x^3 - (1+\theta)x + \theta}{x-1}} y = \sqrt{f(z)} y, \tag{39}$$

where

$$f(z) = e^{2z} + 3e^z + (2 - \theta), \tag{40}$$

we obtain a differential equation which is completely analogous to the uncharged case,

$$\psi'' + V(z)\psi = 0, \tag{41}$$

where

$$V(z) = \frac{\kappa^2}{f} e^z - \frac{f''}{2f} + \left(\frac{f'}{2f} \right)^2. \tag{42}$$

The only change in this equation is that $f(z)$ is altered by the θ term. To perform the WKB analysis we need to find the points where the potential in this equation is zero, as these are the turning points of the WKB approximation. In the limits of large $|z|$, for $\theta \neq 2$, we have

$$V(z) \approx \left[\frac{\kappa^2}{2-\theta} - \frac{3}{2(2-\theta)}\right] e^z \text{ for } z \ll 0, \tag{43}$$

$$V(z) \approx \kappa^2 e^{-z} - 1 \text{ for } z \gg 0. \tag{44}$$

For κ sufficiently large there are thus turning points at $z = -\infty$ and $z = z_0 \approx 2\ln(\kappa)$. The WKB approximation therefore gives

$$\left(n + \frac{1}{2}\right)\pi = \int_{-\infty}^{z_0} dz\sqrt{V(z)}. \tag{45}$$

To leading order in κ we can approximate the integral

$$\left(n + \frac{1}{2}\right)\pi = \int_{-\infty}^{\infty} \kappa\sqrt{\frac{e^z}{f(z)}}dz = \kappa\int_1^{\infty} \frac{dx}{\sqrt{x^3 - (1+\theta)x + \theta}} \equiv \kappa\alpha, \tag{46}$$

where the last equality defines α. The zeros m_n of the Wronskian are thus approximately given by

$$m_n = \frac{\pi}{\alpha}\left(n + \frac{1}{2}\right), \tag{47}$$

where n is a positive integer[2].

In the uncharged case α can be evaluated exactly. For the charged case, we evaluate alpha numerically, and see that as the charge of the black hole is increased, α increases and thus each m_n decreases. In figure 5, we plot the value of the lowest zero m_1 as a function of the parameter θ determining black hole charge. As $\theta \to 2$, α diverges like $\ln(T) \propto \ln(2-\theta)$, where T is the black hole temperature. Since we are obtaining a divergent answer, we should consider the validity of the approximation more carefully.

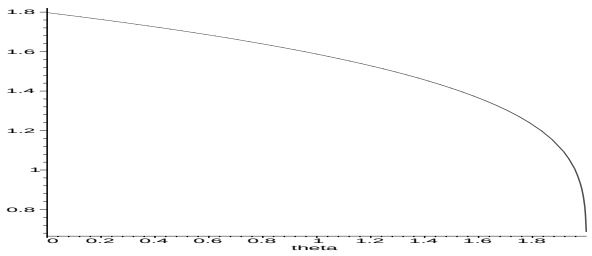

Figure 5: m_1 vs. θ

[2]It is argued in [30] that the extra zero for $n = 0$ does not contribute and this claim is substantiated by comparison to numerical results for calculation of the zeros in the uncharged black hole

The divergence found in the WKB approximation in the extremal case can be explained by considering the potential. For non-extremal black holes the behaviour of $V(z)$ for $z \ll 0$ was as given in (43). This is the case for any value of θ other than 2, but for $\theta = 2$ it is the next term in $f(z)$ which contributes to $V(z)$ for $z \ll 0$. The potential now no longer decays exponentially for $z \ll 0$: instead it becomes constant, and the potential never reaches zero in this region. Therefore there is no second turning point of the equation and the bound state problem has no solutions.

The different nature of the problem in the extremal case was discovered earlier, when we found for equation (32), that the indicial equation for solutions near the black hole horizon is given by $(4-2\theta)(\sigma(\sigma-1)+\sigma) = 0$. This is true for $\theta \neq 2$, but for $\theta = 2$ the dominant terms in the solution near the horizon are those of a lower exponent and they lead to the indicial equation

$$12\sigma(\sigma-1) + 24\sigma - k^2 = 0. \tag{48}$$

For solutions to be well behaved near the horizon this requires $k^2 \geq 0$. This is problematic since the zeros are given by $m^2 = -k^2$. In fact, in the extremal case, (32) can be solved exactly, enabling us to see how it differs from the non-extremal case. Making the substitution $x = u^2$ reduces the homogeneous equation for $\theta = 2$ to

$$(x-1)^2(x+2)\partial_x^2 y + 3(x-1)(x+1)\partial_x y - \frac{k^2}{4}y = 0. \tag{49}$$

Whereas in both the uncharged case and the nonextremal charged case our homogeneous differential equation was linear second order with four regular singularities, this equation only has three regular singularities, at $x = -2$, $x = 1$ and $x = \infty$. We recognise this as the hypergeometric equation and reduce it to the standard form by the transformation $z = 3/(1-x)$. Then

$$z(1-z)\partial_z^2 y - \partial_z y + \frac{k^2}{12}y = 0. \tag{50}$$

We will look for solutions of (50) satisfying our boundary conditions without restricting the sign of k^2, to see if any such solutions exist. We need the solution to be normalizable, so $y \approx u^{-4}$ as $u \to \infty$; after coordinate transformations this condition becomes $y \approx z^2$ as $z \to 0$. We also require the solution to be well-behaved at $u = 1$, i.e., at $z = \infty$. The hypergeometric equation has one solution with the correct behaviour at $z = 0$,

$$y(z) = z^2 F\left(\frac{3}{2}+\lambda, \frac{3}{2}-\lambda, 3; z\right), \quad \lambda = \frac{1}{6}\sqrt{9+3k^2} \geq 0. \tag{51}$$

To examine the behaviour near $z = \infty$, we use the asymptotic expansion in terms of hypergeometric functions in $1/z$ to give

$$\begin{aligned} y(z) &= \frac{\Gamma(3)\Gamma(-2\lambda)}{\Gamma(3/2-\lambda)^2}(-1)^{\frac{3}{2}+\lambda} z^{\frac{1}{2}-\lambda} F\left(\frac{3}{2}+\lambda, -\frac{1}{2}+\lambda, 1+2\lambda; \frac{1}{z}\right) \\ &+ \frac{\Gamma(3)\Gamma(2\lambda)}{\Gamma(3/2+\lambda)^2}(-1)^{\frac{3}{2}-\lambda} z^{\frac{1}{2}+\lambda} F\left(\frac{3}{2}-\lambda, -\frac{1}{2}-\lambda, 1-2\lambda; \frac{1}{z}\right). \end{aligned} \tag{52}$$

Since the hypergeometric function as a function of $1/z$ is asymptotic to 1 at $z = \infty$, for our function to be well-behaved at $z = \infty$ we require that z does not appear outside the hypergeometric function with a positive exponent. In the second term of this expression for $y(z)$ this cannot be achieved, so the gamma function in the denominator must diverge to set this term to zero. However, this would only happen if $3/2 + \lambda = -n$ for n a non-negative integer, and λ is positive. Thus, in the extremal case there are no solutions of the time-independent wave equation satisfying the boundary conditions at both the horizon and the boundary. The breakdown in the WKB analysis near extremality is therefore physical.

In these static propagator calculations, we have found that there is a finite screening length associated with most of the black hole spacetimes. From the calculations in the uncharged black hole, where the screening length is the thermal scale, one might have suspected that this is associated with the thermal fluctuations, which are concealing a divergence in the true behaviour. However, as we increase the charge, the screening length grows only logarithmically in the temperature, and soon falls below the thermal scale. There is thus really some limit on the characteristic scale for probes near the horizon, and we see no sign of a divergent scale size associated with the horizon in this calculation. It also would be interesting to understand the origin of this behaviour in the field theory: since the scale is not simply fixed by the horizon radius U_T, there may be some interesting physics here. From this point of view, it should be stressed that $1/m_n$ only provides an upper bound on the possible scale size; there may be power-law suppression at a smaller scale that this calculation is not sensitive to.

5 Conclusions

We only found signs of the expected divergence in the scale size of dual expectation values for probes near the horizon in the discussion of time-dependent probes. The failure to find such a relationship for Wilson loops is perhaps understandable, since the extended nature of the worldsheet implies that the part of the worldsheet that changes as we vary the asymptotic separation is probing a range of radii near the horizon, and not a specific value. Thus, the Wilson loops do depend non-trivially on the structure of the metric near the horizon, but don't really see the horizon as a horizon.

It is more surprising that static supergravity probes produce dual expectation values with a finite scale size. From the spacetime point of view, this statement means that a point charge close to the horizon produces an asymptotic field which still depends non-trivially on the transverse coordinates x_i. This is quite different from the case of Schwarzschild black holes in flat space, where the field of a charged particle close to the horizon becomes completely spherically symmetric (see [35] and references therein). Note that this is not just the usual difference between the asymptotic behaviours of flat space and AdS: in the Schwarzschild case, the field measured at some finite radius is becoming spherically symmetric as the source approaches the horizon. It would be interesting to know what happens for the Schwarzschild-AdS

solution.

The static propagator also exhibits a mysterious logarithmic dependence on the temperature for small temperatures. It should be noted that this only provides an upper limit for the behaviour of the scale size of excitations for static probes near the horizon, and the actual scale could be constant. Nevertheless, it would be interesting to try to understand this behaviour from the field theory point of view. While no analogue of this behaviour was seen in the glueball mass calculations in rotating backgrounds [19, 20], this should not cause concern. As previously emphasised, these calculations address the physically different Euclidean solution obtained by $t \to i\tau$, $q \to iq'$. In this Euclidean solution, it is not possible to take the temperature to zero; in fact, the minimum value of the temperature is achieved when $q' = 0$.

One interesting example of a 'static' source that is not covered by the foregoing analysis is a D-instanton. To consider a D-instanton, we need to pass to the Euclidean solution, so we cannot really think of it as a probe of the causal structure. However, the expectation value dual to a D-instanton is sensitive to the presence of the horizon in a dramatic way. For non-extremal black holes, the horizon in the Euclidean solution is simply a point where the proper length of the periodic τ direction goes to zero. If we place a D-instanton at this point, the translational symmetry in τ is preserved, so the dual expectation value must be τ-independent. That is, for D-instantons near the horizon, the scale of the dual field theory instanton goes to infinity in the τ direction (and from the above comments on static propagators, in the τ direction only). This may be a useful test for a horizon in the Euclidean solution, but it does not help us to understand the causality of the Lorentzian solution.

The key to a more satisfactory representation of the bulk causal structure may be to develop a relation between the bulk theory and the boundary which does not require us to propagate effects out to the boundary in spacetime. This is difficult to achieve with the present correspondence, as the relation between spacetime and field theory is phrased in terms of boundary conditions on the gravity side. It is worth stressing that this problem is distinct from the problem of studying local physics on scales smaller than the AdS scale; the black holes here can be as large as one wants. Perhaps even resolving this apparently simple question requires the development of a more general background-independent version of the correspondence.

Acknowledgements

We are grateful for discussions with Ian Davies, Clifford Johnson, Esko Keski-Vakkuri, Kenneth Lovis, Don Marolf, Antonio Padilla and David Page. The work of JPG is supported in part by EPSRC studentship 9980045X. JPG thanks the Institut Henri Poincaré for hospitality during the completion of this work.

References

[1] J. Maldacena, "The large N limit of superconformal field theories and supergravity," Adv. Theor. Math. Phys. **2** (1998) 231–252, hep-th/9711200.

[2] S. S. Gubser, I. R. Klebanov, and A. M. Polyakov, "Gauge theory correlators from non-critical string theory," Phys. Lett. **B428** (1998) 105, hep-th/9802109.

[3] E. Witten, "Anti-de Sitter space and holography," Adv. Theor. Math. Phys. **2** (1998) 253–291, hep-th/9802150.

[4] T. Banks, M. R. Douglas, G. T. Horowitz, and E. Martinec, "AdS dynamics from conformal field theory," hep-th/9808016.

[5] V. Balasubramanian, P. Kraus, and A. Lawrence, "Bulk vs. boundary dynamics in anti-de Sitter spacetime," Phys. Rev. D **59** (1999) 046003, hep-th/9805171.

[6] V. Balasubramanian, P. Kraus, A. Lawrence, and S. P. Trivedi, "Holographic probes of anti-de Sitter space-times," Phys. Rev. D **59** (1999) 104021, hep-th/9808017.

[7] V. Balasubramanian and S. F. Ross, "Holographic particle detection," Phys. Rev. D **61** (2000) 044007, hep-th/9906226.

[8] S. B. Giddings and S. F. Ross, "D3-brane shells to black branes on the Coulomb branch," Phys. Rev. D **61** (2000) 024036, hep-th/9907204.

[9] L. Susskind and E. Witten, "The holographic bound in anti-de Sitter space," hep-th/9805114.

[10] A. W. Peet and J. Polchinski, "UV/IR relations in AdS dynamics," Phys. Rev. D **59** (1999) 065011, hep-th/9809022.

[11] J. Distler and F. Zamora, "Non-supersymmetric conformal field theories from stable anti-de Sitter spaces," Adv. Theor. Math. Phys. **2** (1999) 1405, hep-th/9810206.

[12] L. Girardello, M. Petrini, M. Porrati, and A. Zaffaroni, "Novel local CFT and exact results on perturbations of N = 4 super Yang-Mills from AdS dynamics," JHEP **12** (1998) 022, hep-th/9810126.

[13] D. Z. Freedman, S. S. Gubser, K. Pilch, and N. P. Warner, "Renormalization group flows from holography-supersymmetry and a c-theorem," hep-th/9904017.

[14] I. R. Klebanov and E. Witten, "AdS/CFT correspondence and symmetry breaking," Nucl. Phys. **B556** (1999) 89, hep-th/9905104.

[15] D. Kabat and G. Lifschytz, "Gauge theory origins of supergravity causal structure," JHEP **05** (1999) 005, hep-th/9902073.

[16] A. Chamblin, R. Emparan, C. V. Johnson, and R. C. Myers, "Charged AdS black holes and catastrophic holography," Phys. Rev. D **60** (1999) 064018, hep-th/9902170.

[17] A. Chamblin, R. Emparan, C. V. Johnson, and R. C. Myers, "Holography, thermodynamics and fluctuations of charged AdS black holes," Phys. Rev. D **60** (1999) 104026, hep-th/9904197.

[18] S. W. Hawking and H. S. Reall, "Charged and rotating AdS black holes and their CFT duals," Phys. Rev. D **61** (2000) 024014, hep-th/9908109.

[19] C. Csaki, Y. Oz, J. Russo, and J. Terning, "Large N QCD from rotating branes," Phys. Rev. D **59** (1999) 065012, hep-th/9810186.

[20] J. G. Russo and K. Sfetsos, "Rotating D3 branes and QCD in three dimensions," Adv. Theor. Math. Phys. **3** (1999) 131, hep-th/9901056.

[21] A. Brandhuber, N. Itzhaki, J. Sonnenschein, and S. Yankielowicz, "Wilson loops in the large N limit at finite temperature," Phys. Lett. **B434** (1998) 36–40, hep-th/9803137.

[22] S.-J. Rey, S. Theisen, and J.-T. Yee, "Wilson-Polyakov loop at finite temperature in large N gauge theory and anti-de Sitter supergravity," Nucl. Phys. **B527** (1998) 171, hep-th/9803135.

[23] S.-J. Rey and J. Yee, "Macroscopic strings as heavy quarks in large N gauge theory and anti-de Sitter supergravity," hep-th/9803001.

[24] J. Maldacena, "Wilson loops in large N field theories," Phys. Rev. Lett. **80** (1998) 4859–4862, hep-th/9803002.

[25] J. Sonnenschein, "What does the string / gauge correspondence teach us about Wilson loops?," hep-th/0003032.

[26] D. Z. Freedman, S. S. Gubser, K. Pilch, and N. P. Warner, "Continuous distributions of D3-branes and gauged supergravity," JHEP **07** (2000) 038, hep-th/9906194.

[27] A. Brandhuber and K. Sfetsos, "Wilson loops from multicentre and rotating branes, mass gaps and phase structure in gauge theories," hep-th/9906201.

[28] E. Witten, "Anti-de Sitter space, thermal phase transition, and confinement in gauge theories," Adv. Theor. Math. Phys. **2** (1998) 505, hep-th/9803131.

[29] A. Brandhuber, N. Itzhaki, J. Sonnenschein, and S. Yankielowicz, "Wilson loops, confinement, and phase transitions in large N gauge theories from supergravity," JHEP **06** (1998) 001, hep-th/9803263.

[30] U. H. Danielsson, E. Keski-Vakkuri, and M. Kruczenski, "Vacua, propagators, and holographic probes in AdS/CFT," JHEP **01** (1999) 002, hep-th/9812007.

[31] G. T. Horowitz and N. Itzhaki, "Black holes, shock waves, and causality in the AdS/CFT correspondence," JHEP **02** (1999) 010, hep-th/9901012.

[32] M. Banados, C. Teitelboim, and J. Zanelli, "The black hole in three-dimensional space-time," Phys. Rev. Lett. **69** (1992) 1849–1851, hep-th/9204099.

[33] C. Csaki, H. Ooguri, Y. Oz, and J. Terning, "Glueball mass spectrum from supergravity," JHEP **01** (1999) 017, hep-th/9806021.

[34] J. A. Minahan, "Glueball mass spectra and other issues for supergravity duals of QCD models," JHEP **01** (1999) 020, hep-th/9811156.

[35] D. A. Macdonald, R. H. Price, W.-M. Suen, and K. S. Thorne, "Nonrotating and slowly rotating black holes," in *Black holes: the membrane paradigm*, R. H. P. Kip S. Thorne and D. A. Macdonald, eds., p. 13. Yale University Press, New Haven, USA, 1986.